Three-Dimensional Model and Molecular Dynamics Simulation of the Active Site of the Self-Splicing Intervening Sequence of the Bacteriophage T4 *nrdB* Messenger RNA†

Lennart Nilsson,*,‡ Agneta Åhgren-Stålhandske,§ Ann-Sofie Sjögren,§ Solveig Hahne,§ and Britt-Marie Sjöberg§
Department of Medical Biophysics, Karolinska Institutet, S-104 01 Stockholm, Sweden, and Department of Molecular Biology, University of Stockholm, S-106 91 Stockholm, Sweden

Received April 12, 1990; Revised Manuscript Received July 10, 1990

ABSTRACT: The secondary and 3D structure of the active site of the self-splicing T4 *nrdB* RNA has been modeled on a graphics workstation by use of the suggested 3D arrangement of the active site of the *Tetrahymena* IVS [Kim, S. H., & Cech, T. R. (1987) *Proc. Natl. Acad. Sci. U.S.A. 84*, 8788–8792] as a guideline. The initially obtained crude structure was then subjected to molecular mechanics energy minimization and molecular dynamics simulation to relax tensions. In this process the energy decreased considerably and gave a final structure that deviated by 3 Å [root mean square (rms)] from the initial structure. The cofactor guanosine (and the competitive inhibitor arginine) was docked to a proposed [Michel, F., Hanna, M., Green, R., Bartel, D. P., & Szostak, J. W. (1989) *Nature 342*, 391–395] binding site, where it was found to fit rather well. A minor modification of the binding mode easily brought the O3′ end of the guanosine within 2 Å of the phosphodiester bond where the primary cleavage occurs.

The bacteriophage T4 gene coding for the small subunit of the phage-specific enzyme ribonucleotide reductase contains a group IA self-splicing intron of 598 nt (Sjöberg et al., 1986; Gott et al., 1986). Two other self-splicing introns of the same type are found in the T4 genome, the 1016-nt intron in the *td* gene (Chu et al., 1984) and the 1033-nt intron in the *sunY* gene (Shub et al., 1988b). With variable occurrence these three introns may also be found in other related *Escherichia coli* T-even phages (Pedersen-Lane et al., 1987; Quirk et al., 1989). Recently, Shub et al. (1988a) discovered an 883-nt self-splicing intron in the DNA polymerase gene of bacteriophage SPOI, which infects the Gram-positive bacterium *Bacillus subtilis*. The group IA class of introns also includes 15 self-splicing introns from fungal mitochondrial and chloroplast genomes (Cech, 1988).

The interest in and knowledge of self-splicing introns have grown exponentially over the last few years, and to date more than 70 introns have been classified as group I or IA according to their predicted secondary structure [for a classification of self-splicing introns, see Burke et al. (1987)]. Of these, approximately 11 have been shown to be self-splicing in vitro (Cech, 1988). Several investigators have used random or directed mutagenesis to corroborate the predictions of the hypothetical secondary structure and to minimize the introns to the smallest catalytic entity. Along these lines, a 335-nt 5′ part (Barfod & Cech, 1989), a 69-nt internal deletion (Joyce et al., 1989) of the *Tetrahymena* intron, and a 305-nt construction of the T4 *sunY* intron (Xu & Shub, 1989) have all been shown to be self-splicing in vitro. Catalysis of 5′ exon cleavage is retained in a 184-nt derivative of the *sunY* intron (Doudna & Szostak, 1989).

Many of the secondary predictions of the 413-nt *Tetrahymena* intron have been corroborated by site-specific cleavages and chemical modifications. Kim and Cech (1987) presented a hypothetical three-dimensional model of the active site of the *Tetrahymena* intron based on principles of RNA folding derived from a crystallographic structure of $tRNA^{Phe}$ (Kim, 1979). Recently Latham and Cech (1989) used the efficient hydroxyl radical cleavage of nucleic acids to obtain extensive hydrolysis of the intron and found that certain areas of the intron were refractory to cleavage. On the basis of this study, Latham and Cech defined sequences located to the inside of the intron and could conclude that much of the three-dimensional predictions of the *Tetrahymena* intron were borne out by the chemical cleavage test. Michel et al. (1989) were able in a recent study to identify the parts of the active site of the intron that recognize the guanosine cofactor which initiates the 5′ cleavage reaction.

It is likely that the three-dimensional structures of the catalytic site of self-splicing introns will have several common features, especially given the high homology between secondary structural elements of group I and group IA introns. We have therefore extended the studies of Cech and co-workers (Kim & Cech, 1987; Latham & Cech, 1989) by model building the structural elements of the *nrdB* intron into the proposed structural model of the *Tetrahymena* active site and subsequently performed a molecular dynamics simulation with the model of the T4 *nrdB* intron. A molecular dynamics simulation gives a more efficient relaxation of the model than can be achieved by energy minimization and also provides some insight into the stability and flexibility of the various parts of the model.

Materials and Methods

Molecular Dynamics (MD) Simulations. All molecular dynamics simulations were performed on a CONVEX C-210 computer using the program CHARMM (Brooks et al., 1983) with energy parameters for nucleic acids (Nilsson & Karplus, 1986) and the standard CHARMM protein energy parameters with explicit hydrogen bonds (Brooks et al., 1983) for the arginine inhibitor. A total of 111 "hydrated" sodium ions were included in the simulations, as described by Singh et al. (1985), yielding a total of 2822 atoms with guanosine or 2816 atoms with arginine ligands. The counterions were allowed to move

† This work was supported by grants from the Swedish Natural Science Research Council, the Lisa and Johan Grönberg Foundation, the Knut and Alice Wallenberg Foundation, the O. E. and Edla Johansson Scientific Foundation, and the Magnus Bergvall Foundation.

‡ Karolinska Institutet.
§ University of Stockholm.

0006-2960/90/0429-10317$02.50/0

but prevented from escaping by a quartic restoring potential centered at the center of mass of the system, with a force constant selected to give the ions an energy of approximately 0.5 kT at a distance of 40 Å (Post et al., 1986).

The ends of the (artificially) cut helices P4, P6, and P7, as well as the base pairs G_{500}-C_{36} and U_{41}-G_{495} at the ends of P3, were further kept from fraying by the addition of harmonic constraints to keep the Watson–Crick base pairing intact.

Structures were initially energy minimized for 100 steepest descent steps followed by 1000 steps with the adopted-basis Newton Raphson (ABNR) method (Brooks et al., 1983), together with "soft" harmonic constraints on the atom positions, which were updated to use the current positions as reference positions every 50 steps, and with gradually decreasing force constants from 50 to 5 kcal mol^{-1} $Å^{-2}$.

The molecular dynamics simulations were performed with a time step of 2 fs using Langevin dynamics, with a friction coefficient corresponding to the viscosity of water (50 ps^{-1}), and with a dielectric permittivity $\epsilon = r$, the interatomic distance expressed in angstroms. The simulations were started by assigning velocities to all atoms from a Gaussian distribution corresponding to a temperature of 100 K and increasing the temperature to 500 K by reassigning the velocities every 100 steps.

Average structures were calculated for the 5–10-, 25–30-, 30–50-, and 45–50-ps periods, and the final average was subjected to 1000 steps of ABNR energy minimization. The arginine inhibitor was docked to the 45–50-ps average structure, and the new complex was again energy minimized for 1000 steps.

Initial MD simulations, without the counterions and without the Langevin friction and thermal bath, rapidly caused severe deformations (data not shown) of the whole system and prompted us to add in the friction and the thermal bath.

Molecular Graphics. The building of the three-dimensional arrangement of the helices, the placement of joining single-stranded segments, and the docking of the arginine and guanosine cofactors were performed with the program HYDRA (Polygen, Waltham, MA) on an IRIS 3120 workstation (Silicon Graphics Inc., Mountain View, CA). Single-stranded segments were built by sequential docking of single nucleotides, torsion angles of the nucleotides being adjusted as necessary, from both ends of the stretch that was to be spanned rather than attempting to put the whole segment in place by manipulations of torsion angles of several nucleotide units simultaneously.

Results and Discussion

Initial Structure. The initial three-dimensional model of the T4 *nrdB* intron was based on the secondary structure model of Shub et al. (1988a). The *nrdB* intron belongs to the group IA subset (Burke et al., 1987) of self-splicing introns. A two-dimensional arrangement of the secondary structure regions P1, P2, P3, P4, P6, P7, and P8 was constructed (Figure 1) on the basis of the *Tetrahymena* IVS model suggested by Kim and Cech (1987). Differences as compared to the proposed secondary structure include the U_{494}-A_{521} base pair between the 3′ part of P3 and the 3′ part of P7 (Figure 1). Helical segments consisting of regions P1/P2, P7/P3/P8, and P4/P6 were then generated with A-RNA helix parameters (Arnott et al., 1975) and arranged in three dimensions (Figure 2) as suggested by Kim and Cech (1987). During the molecular graphics building of the initial arrangement, which was based on maximal base pairing, it was found that the connecting single-stranded segment between P7 and P8 had to be lengthened from three to five nucleotides in order to span

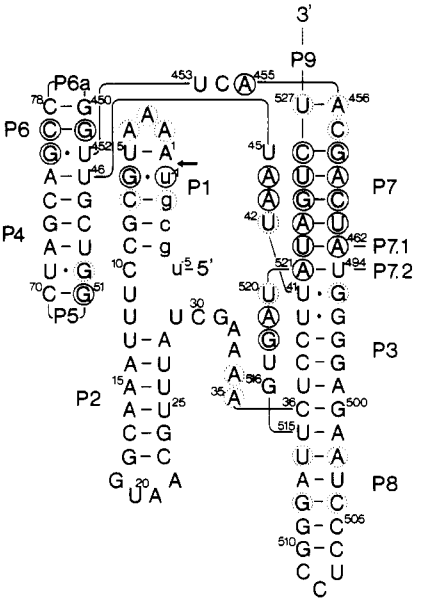

FIGURE 1: Secondary structure model of the *nrdB* IVS with helical elements positioned according to Shub et al. (1988a) and Kim and Cech (1987). Filled circles denote highly conserved nucleotides within group I and IA introns; dotted circles denote nucleotides conserved only among the bacteriophage T4 introns.

the six base pair long P3 helix. This type of modification is in agreement with the theoretical considerations of Kim and Cech (1987) for the requirements of the stacked P7/P3/P8 helical segment.

The cofactor guanosine was initially docked to the splice site in P1 in two ways: first with the guanosine base close to the base pair U_{-1}-G_6, which was rearranged to allow the formation of a hydrogen-bonded base triplet as suggested by Inoue et al. (1986), and second in a fashion proposed by Michel et al. (1989) with the guanosine base interacting with the base pair G_{458}-C_{526} in helix P7. Both of these structures were energy minimized and simulated for 50 ps.

The first mode of binding leaves the 3′-hydroxyl group of the cofactor 13 Å from the actual cleavage site in P1, and the MD simulation did not bring it any closer than 10 Å, even though an extra harmonic potential had been included in this run in order to pull the cofactor 3′ end close to the cleavage site. This simulation was therefore discarded in the final analysis presented below, where only data pertaining to the structure with the cofactor docked according to Michel et al. (1989) are used.

Energy-Minimized and Molecular Dynamics Average Structures vs Initial Structure. The energy minimization relieved the worst clashes that had been introduced in the crude modeling, thus dramatically decreasing the energy of the system, with a small change in the overall structure. During the course of the MD simulation the structure continued to relax (Figure 3), increasing the overall rms deviation from the initial model-built structure to 3 Å. The potential and kinetic energies of the system during the MD simulation shown in Figure 4 indicate that the system has stabilized energetically as well as structurally (Figure 3) at the end of the 50 ps. The kinetic energy of 3880 kcal/mol corresponds to a temperature of 480 K.

The majority of the nucleotides remained within 2–3 Å of their starting positions (Figure 5), with a small increase in deviation per nucleotide toward the end of the simulation. Nucleotides C_9, A_{34}, U_{494}, and G_{496} are the ones that deviate the most (>4.5 Å), whereas nucleotides U_{26}, A_{456}, and C_{457} show the smallest deviations (<1.2 Å).

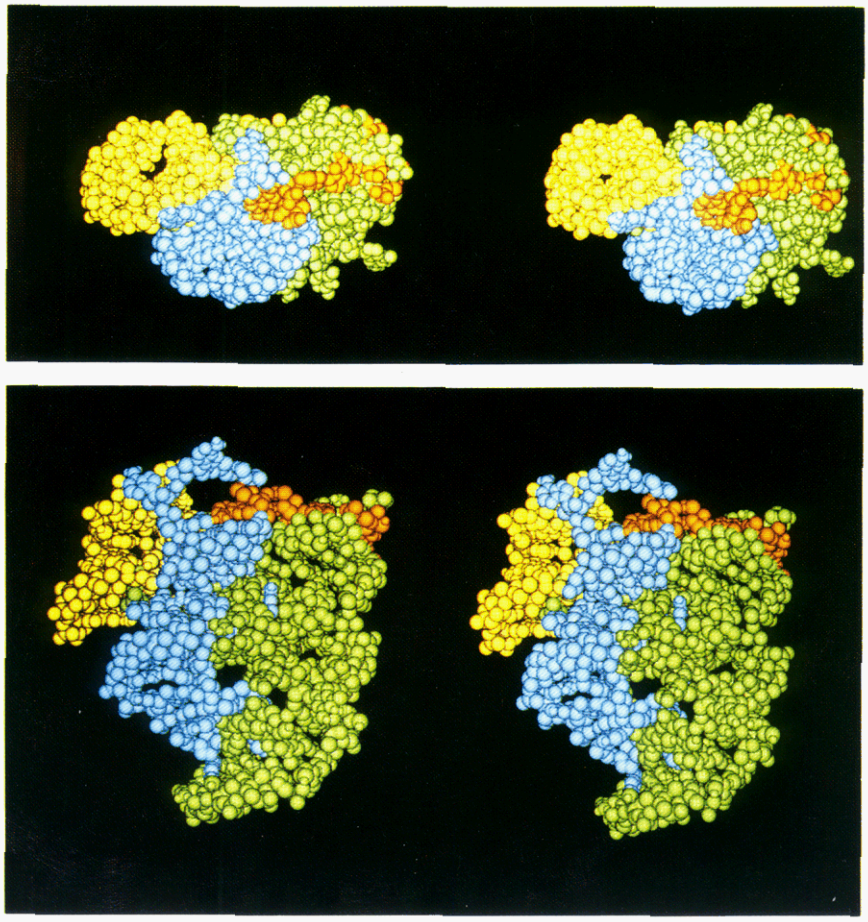

FIGURE 2: Stereoviews of the three-dimensional model, showing helices P1/P2 in blue, P7/P3/P8 in green, and P4/P6 in yellow. The guanosine cofactor and nucleotides U_{-1}, A_1, G_{458}, and C_{526} are in red. (Top) Top view; (bottom) front view.

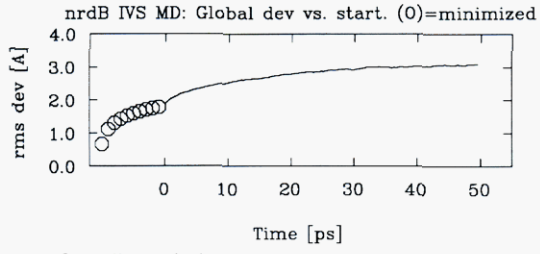

FIGURE 3: Overall rms deviation from the initial structure as a function of time in the MD simulation. The circles at negative time represent intermediate structures in the initial minimization (separated by 100 minimization cycles).

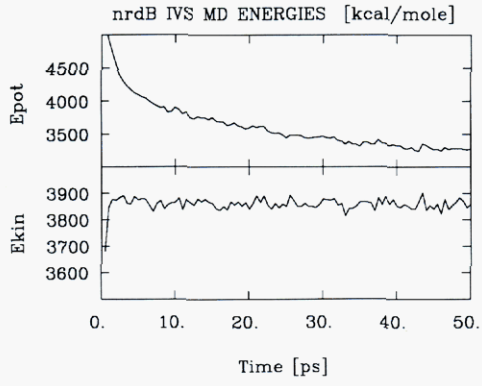

FIGURE 4: Potential and kinetic energy as a function of time in the MD simulation.

A closer examination of the individual helices reveals that although they all retain their helical character and overall shape, there are small readjustments of nucleotide positions

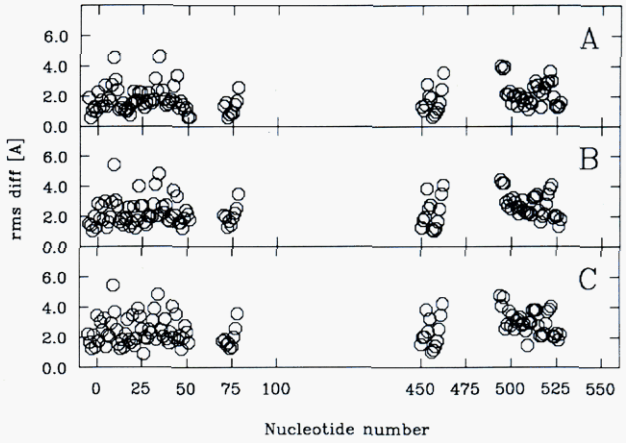

FIGURE 5: rms atomic displacement, averaged per nucleotide, between the MD average structures and the initial model as a function of residue number: (A) average from 5 to 10 ps; (B) average from 25 to 30 ps; (C) average from 45 to 50 ps.

and base pairs within the helices, still leaving the overall helical structure intact and in place relative to the other elements in the system. One example is A_{521}, which in the final structure has turned almost 90° so that it no longer is stacked between helices P3 and P7. This is not too surprising since this is one of the stress points in the structure, where the phosphate backbone leaves helix P7 and continues as a single strand past P3 before joining P8 again (Figure 1).

The initial structure was built with just the main features (i.e., the arrangement of secondary structure elements relative to each other) of the model proposed by Kim and Cech (1987), without regard to a number of tertiary base pairs that were

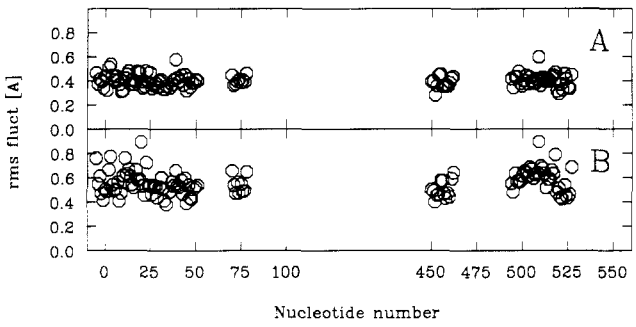

FIGURE 6: rms fluctuations around the average structure, averaged per nucleotide, as a function of nucleotide number for different averaging periods: (A) 45–50 ps; (B) 30–50 ps.

Table I: Closest Distances (≤5 Å) between Guanosine Cofactor and Neighboring Nucleotides

cofactor	IVS nucleotide	distance (Å)
sugar		
H3T[a]	U_{-1}(O3′)[b]	2.0
H3T	A_1(C5′)	2.8
O5′	A_{456}(O1P)	3.0
O2′	A_{523}(O2P)	3.4
C2′	G_{524}(O1P)	4.6
O5′	A_{455}(O3′)	4.7
base		
O6	C_{526}(H41)	1.7
H21	C_{457}(H41)	1.9
H1	G_{458}(O6)	2.7
C2	A_{456}(H62)	2.8
O6	U_{525}(O4)	2.9
H1	A_{459}(H62)	3.6
H1	U_{527}(O4)	4.1
C8	G_{524}(O1P)	4.2

[a] H3T is the 3′-hydroxyl hydrogen atom. [b] Boldface denotes nucleotides that are highly conserved within group I and group IA introns.

also suggested for the *Tetrahymena* system. Only two of these actually have correspondence in the *nrdB* system (A_{455}-U_{45} and U_{494}-A_{521}), but they are not formed in the dynamics average structure, apparently without any detrimental effects on the global structure.

Fluctuations. The atomic rms fluctuations around their mean positions (averaged per nucleotide) are shown as a function of nucleotide position in Figure 6. The relatively uniform pattern, with a magnitude typical of macromolecular simulations, indicates that there are neither any very loose nor any very tightly packed regions in the system. The larger rms values obtained for the longer averaging period are also what is expected and may in part be due to the small remaining structural drift from 30 to 50 ps which is also seen in Figure 3.

Active Site with Guanosine Cofactor. The suggestion by Michel et al. (1989) that the cofactor interacts with a base pair at the end of helix P7 in the group I *Tetrahymena* IVS was carried over to the group IA *nrdB* IVS model. In the *nrdB* system the guanosine should form hydrogen bonds to G_{458}, which is base paired to C_{526}, at the corresponding location in helix P7. This brought the O3′ of the cofactor within 5 Å of the site of the initial cleavage reaction in helix P1 at the phosphodiester bond between A_1 and U_{-1}, without any need for further modifications of the model. To obtain close contact (≈3 Å) between the G-O3′ and the U_{-1}-O3′, the cofactor was repositioned slightly in such a way that the hydrogen bond G-N2–G_{458}-N7 is replaced by hydrogen bond G-O6–C_{526}-N4 (Figure 7A). During the MD simulation the guanosine moved even closer, by 1 Å, to the cleavage site at the expense of losing its hydrogen bond to G_{458} (Figure 7B). The guanosine also rotated slightly and moved a little bit out of the plane of G_{458} and C_{526}, increasing its interactions somewhat with other nearby nucleotides. The IVS nucleotides within 5 Å of the guanosine are listed in Table I, and it can be seen that (apart from G_{458} and C_{526}) C_{457}, A_{456}, and U_{525} are the ones that are closest to the guanosine base with A_{456} being close to the guanosine ribose as well. Of these, U_{525} is conserved within group I and group IA (Cech, 1988).

Table II: Interaction Energies (kcal/mol) between Ligands and *nrdB* IVS Nucleotides or Ions within 7 Å

	ETOT	van der Waals	electrostatic	H-bond
Interactions with GUA Cofactor				
nucleotide				
all	−41.0	−23.9	−7.9	−9.2
A_{455}	0.9	−0.0	0.9	0.0
A_{456}	−4.5	−2.5	−0.7	−1.3
C_{457}	0.1	−1.2	1.3	0.0
G_{458}[a]	0.9	−0.2	1.2	0.0
A_{459}	0.1	−0.2	0.2	0.0
C_{460}	0.3	−0.0	0.4	0.0
U_{522}	0.5	−0.1	0.7	0.0
A_{523}	−7.9	−1.9	−4.3	−1.7
G_{524}	−1.4	−2.8	1.4	0.0
U_{525}	1.0	−1.2	2.2	0.0
C_{526}	0.8	−1.6	2.4	−0.0
U_{527}	−10.7	−1.5	−7.2	−1.9
G_{-2}	0.5	−0.0	0.5	0.0
U_{-1}	−10.4	−1.1	−6.0	−3.2
A_1	−4.3	−3.4	0.0	−0.9
A_2	−0.1	−0.3	0.2	0.0
ions				
I_1	−2.6	−0.8	−1.8	0.0
I_3	−2.0	−2.0	−0.0	0.0
I_{77}	−1.6	−1.4	−0.2	0.0
I_{78}	−0.8	−1.2	0.3	0.0
Interactions with ARG Inhibitor				
nucleotide				
all	−30.4	−22.1	−2.9	−5.3
A_{455}	2.6	−0.1	2.8	0.0
A_{456}	−2.4	−2.6	0.1	0.0
C_{457}	−0.4	−3.8	3.3	−0.0
G_{458}	−13.9	−1.2	−9.4	−3.2
A_{459}	1.5	−1.0	2.5	0.0
C_{460}	0.9	−0.0	1.0	0.0
U_{522}	−1.2	−0.4	−0.8	0.0
A_{523}	−16.4	−3.7	−10.7	−1.9
G_{524}	−1.4	−0.4	−1.0	0.0
U_{525}	−1.3	−0.5	−0.7	−0.0
C_{526}	3.8	−0.9	4.7	0.0
U_{527}	−2.7	−0.9	−1.7	−0.0
G_{-2}	−0.9	−0.0	−0.9	0.0
U_{-1}	−4.3	−1.6	−2.6	−0.1
A_1	0.8	−0.6	1.4	0.0
A_2	1.2	−0.0	1.2	0.0
ions				
I_1	0.3	−0.7	1.1	0.0
I_3	3.6	−1.5	5.2	0.0
I_{77}	4.7	−0.2	5.0	0.0
I_{78}	0.7	−0.0	0.7	0.0

[a] Boldface denotes nucleotides that are highly conserved within group I and group IA introns.

The phosphate group at the cleavage site in helix P1 is in a normal tetrahedral conformation with the ζ (O3′–P) and α (P–O5′) torsion angles in g^- conformations as is typical for RNA (Saenger, 1984).

Active Site with Arginine Inhibitor. The final MD average structure of the IVS–Gua complex was used as a docking target (with the guanosine cofactor removed) for an arginine inhibitor (Yarus, 1988). The arginine replaced the guanosine in a similar way as proposed by Michel et al. (1989), with hydrogen bonds between the two amino groups of the arginine side chain and the G_{458} N7 and O6 atoms. This positions the arginine NH_3^+ close to the U_{-1} phosphate group, thus creating

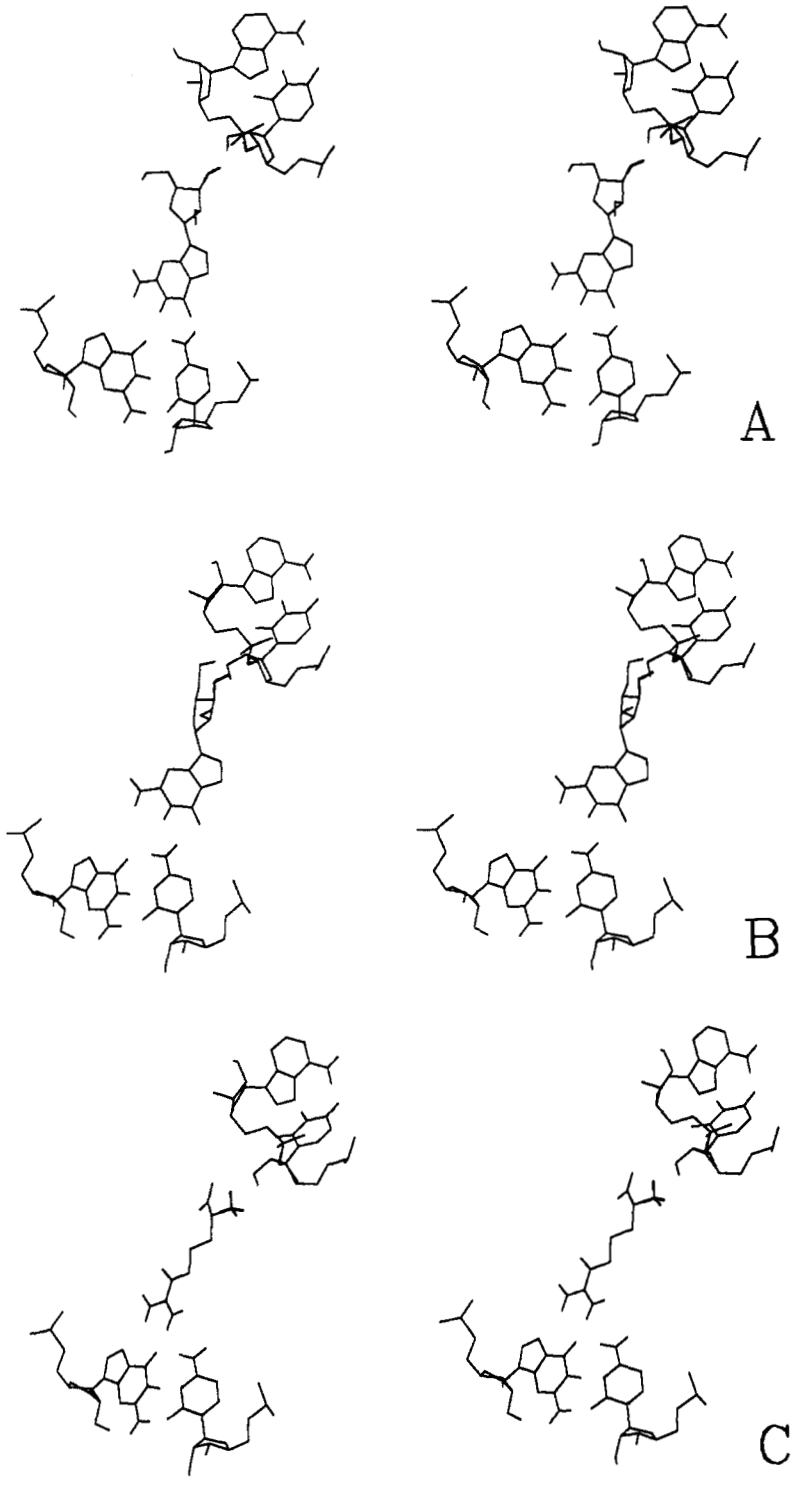

FIGURE 7: Stereo drawings of the active site of the *nrdB* IVS with (A) the guanosine cofactor in its initial position, (B) with the guanosine after MD simulation and minimization, and (C) with an arginine interacting with G_{458}-C_{526} after energy minimization.

a stabilizing electrostatic interaction between the arginine and the RNA. This interaction is, however, not specific for arginine since it does not involve the side chain.

Interaction Energetics. The interaction energies between the nucleotides close to the active site and the G or Arg ligands, respectively, were calculated to give some indication of which interactions are the most important in stabilizing the complex.

The interaction energies $E_{IVS-Arg}$ and $E_{IVS-Gua}$, calculated for the interaction between ligand and all intron (IVS) nucleotides or ions within 7.0 Å of the ligand, are presented in Table II, where the energy has been broken up into its van der Waals, electrostatic, and hydrogen-bond components. It can be seen that all the van der Waals energies are negative, indicating that there are no bad contacts in this region of either structure. The total interaction is somewhat more favorable for the guanosine, mainly due to electrostatic interactions with the counterions in the vicinity of the active site. This is qualitatively to be expected from the measured K_m (μM) and K_i (mM) values for guanosine and arginine, respectively, in a group I intron system (Hicke et al., 1989). In the majority of cases the total interaction energies are very close, but in a few instances there are significant differences (>4 kcal/mol): U_{-1} and A_1 at the cleavage site favor the guanosine over the arginine, as does U_{527}, whereas nucleotides G_{458} and A_{523} have more favorable interactions with the arginine (Table II; Figure 7A,C).

P1 Attachments. It has been proposed (Kim & Cech, 1987) that the helix P1 is attached to the single-stranded regions G_{516}**UGA**U_{520} and U_{42}**AA**U_{45} (nucleotides in boldface are conserved in group I and group IA), which are indeed in direct contact with P1 in the present model. A_{44} is hydrogen bonded to U_{-1}; U_{520} is hydrogen bonded to G_{-4} and to the sugar of C_{10}. There are also hydrogen bonds from G_{518} and A_{519} to the sugar and phosphate of the nucleotides $C_{10}U_{11}U_{12}$ at the end of helix P1 (Figure 1).

CONCLUSIONS

A computer-built model of a large RNA, consisting of three extended helices in the core of the self-splicing intron of the T4 *nrdB* gene, forms a stable structure which can be used to study interactions with various ligands. There is indeed a suitable cavity between helices P1 and P7 in which the cofactor guanosine, necessary for the splicing reaction, fits nicely, as does the inhibitor arginine. The geometry of this active site is such that the ligands form specific contacts with nucleotides in helix P7, in accordance with studies on the *Tetrahymena* intron by Michel et al. (1989), while maintaining a close contact between the reacting groups of the intron and the guanosine.

ACKNOWLEDGMENTS

We are grateful to the Department of Molecular Genetics, Karolinska Institutet, and to Dr. Ulf Skoglund for the use of their CONVEX C210 computer.

Registry No. Guanosine, 118-00-3; L-arginine, 74-79-3.

REFERENCES

Arnott, S., Campbell Smith, P. J., & Chandrasekaran, R. (1975) in *Handbook of Biochemistry and Molecular Biology* (Fasman, G. D., Ed.) p 419, CRC Press, Cleveland, OH.

Barfod, E. T., & Cech, T. R. (1988) *Genes Dev. 2*, 652.

Brooks, B. R., Bruccoleri, R. E., Olafson, B. D., States, D. J., Swaminathan, S., & Karplus, M. (1983) *J. Comput. Chem. 4*, 187.

Burke, J. M., Belfort, M., Cech, T. R., Davies, R. W., Schweyen, R. J., Shub, D. A., Szostak, J. W., & Tabak, H. F. (1987) *Nucleic Acids Res. 15*, 7217.

Cech, T. R. (1988) *Gene 73*, 259.

Chu, F. K., Maley, G. F., Maley, F., & Belfort, M. (1984) *Proc. Natl. Acad. Sci. U.S.A. 81*, 3049.

Doudna, J. A., & Szostak, J. W. (1989) *Mol. Cell. Biol. 9*, 5480.

Gott, J. M., Shub, D. A., & Belfort, M. (1986) *Cell 10*, 81.

Hicke, B. J., Christian, E. L., & Yarus, M. (1989) *EMBO J. 8*, 3843.

Inoue, T., Sullivan, F. X., & Cech, T. R. (1986) *J. Mol. Biol. 189*, 143.

Joyce, G. F., van der Horst, G., & Inoue, T. (1989) *Nucleic Acids Res. 17*, 7879.

Kim, S. H. (1979) in *TRANSFER RNA: Structure, Properties, and Recognition* (Schimmel, P., Söll, D., & Abelson, J., Eds.) pp 83–100, Cold Spring Harbor Laboratory, Cold Spring Harbor, NY.

Kim, S. H., & Cech, T. R. (1987) *Proc. Natl. Acad. Sci. U.S.A. 84*, 8788.

Latham, J. A., & Cech, T. R. (1989) *Science 245*, 276.

Michel, F., Hanna, M., Green, R., Bartel, D. P., & Szostak, J. W. (1989) *Nature 342*, 391.

Nilsson, L., & Karplus, M. (1986) *J. Comput. Chem. 7*, 591.

Pedersen-Lane, J., & Belfort, M. (1987) *Science 237*, 182.

Post, C. B., Brooks, B. R., Dobson, C. M., Artymiuk, P., Cheetham, J., Phillips, D. C., & Karplus, M. (1986) *J. Mol. Biol. 190*, 455.

Quirk, S. M., Bell-Pedersen, D., Tomaschewski, J., Rueger, W., & Belfort, M. (1989) *Nucleic Acids Res. 17*, 301.

Saenger, W. (1984) *Principles of Nucleic Acid Structure*, Springer-Verlag, New York.

Shub, D. A., Goodrich, H. A., Gott, J. M., Xu, M. Q., & Scarlato, V. (1988a) *J. Cell. Biochem. 12D* (Suppl.), 30.

Shub, D. A., Gott, J. M., Xu, M. Q., Lang, B. F., Michel, F., Tomaschewski, J., Pedersen-Lane, J., & Belfort, M. (1988b) *Proc. Natl. Acad. Sci. U.S.A. 85*, 1151.

Singh, U. C., Weiner, S. J., & Kollman, P. (1985) *Proc. Natl. Acad. Sci. U.S.A. 82*, 755.

Sjöberg, B. M., Hahne, S., Mathews, C. Z., Mathews, C. K., Rand, K. N., & Gait, M. J. (1986) *EMBO J. 5*, 2031.

Xu, M. Q., & Shub, D. A. (1989) *Gene 82*, 77.

Yarus, M. (1988) *Science 240*, 1751.